

Doubly-Universal Adversarial Perturbations: Deceiving Vision-Language Models Across Both Images and Text with a Single Perturbation

Hee-Seon Kim* Minbeom Kim* Changick Kim
 Korea Advanced Institute of Science and Technology (KAIST)
 {hskim98, alsqja1754, changick}@kaist.ac.kr

Abstract

Large Vision-Language Models (VLMs) have demonstrated remarkable performance across multimodal tasks by integrating vision encoders with large language models (LLMs). However, these models remain vulnerable to adversarial attacks. Among such attacks, Universal Adversarial Perturbations (UAPs) are especially powerful, as a single optimized perturbation can mislead the model across various input images. In this work, we introduce a novel UAP specifically designed for VLMs: the Doubly-Universal Adversarial Perturbation (Doubly-UAP), capable of universally deceiving VLMs across both image and text inputs. To successfully disrupt the vision encoder’s fundamental process, we analyze the core components of the attention mechanism. After identifying value vectors in the middle-to-late layers as the most vulnerable, we optimize Doubly-UAP in a label-free manner with a frozen model. Despite being developed as a black-box to the LLM, Doubly-UAP achieves high attack success rates on VLMs, consistently outperforming baseline methods across vision-language tasks. Extensive ablation studies and analyses further demonstrate the robustness of Doubly-UAP and provide insights into how it influences internal attention mechanisms.

1. Introduction

Large Vision-Language Models (VLMs) [5, 24, 25] have emerged as powerful tools for tasks requiring both visual and textual understanding, such as image classification, image captioning, and visual question answering (VQA) [12, 27, 35]. By combining vision encoders from vision-language pertaining models [33, 37] with large language models (LLMs) [3, 38], VLMs achieve remarkable performance in multimodal tasks. However, as these models are increasingly deployed in critical applications, concerns about their robustness to adversarial attacks become more pressing.

*Equal contribution.

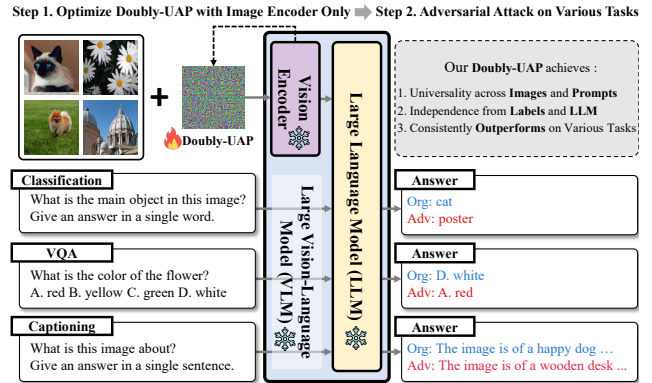


Figure 1. **Overview of the Doubly-UAP Attack on Vision-Language Models.** (Step 1) We optimize the Doubly-UAP on the vision encoder alone, while LLM remains a black-box. (Step 2) The Doubly-UAP successfully deceives the VLM across diverse image and text inputs.

Adversarial attacks are techniques that generate perturbations added to images, which are imperceptible to humans but can significantly mislead the model’s judgment [7, 8, 11, 17, 21, 48]. Among these, Universal Adversarial Perturbations (UAPs) [13, 15, 18, 23, 29–31, 51, 52] are particularly effective, as they can deceive models across various inputs using a single optimized perturbation. Once a UAP is created, it can be applied to any unseen image without additional optimization. This makes UAP highly practical than image-specific adversarial attack methods, which must generate a new perturbation each time the input image changes. While some studies have explored optimizing a single image to mislead VLMs under diverse text inputs [4, 28, 32, 34, 40, 55], there is currently no research focusing on crafting a single UAP that effectively deceives VLMs across multiple images. This is mainly due to the complexity of creating a robust single perturbation that generalizes well, in spite of its effectiveness.

In our work, we aim to generate UAPs specifically designed for VLMs as shown in Fig. 1. A successful UAP should effectively distort the visual information itself. We assume that such a UAP hinders responses to text inputs

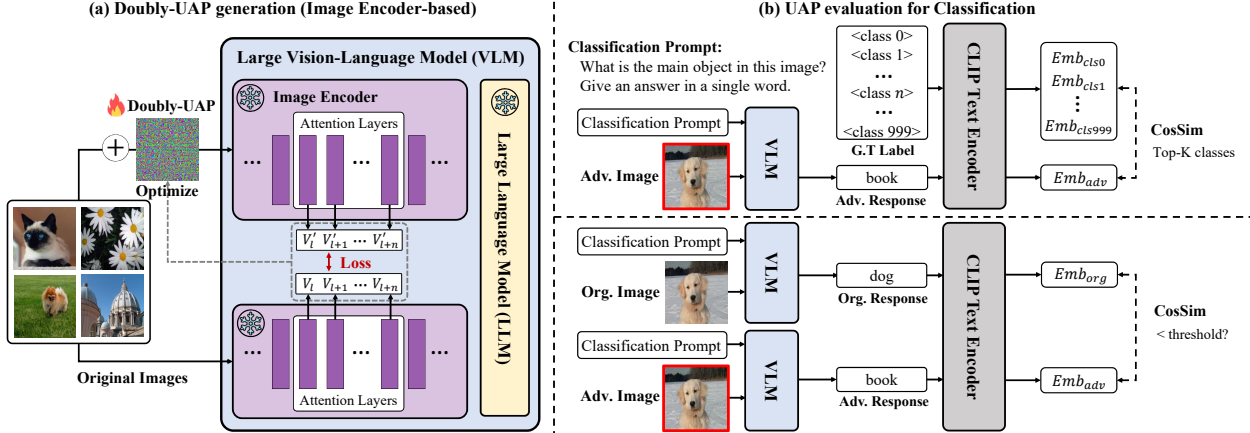


Figure 2. **Overview of Doubly-UAP Creation and Evaluation on Vision-Language Models (VLMs).** (a) The Doubly-UAP is generated by specifically targeting and disrupting the internal attention components (e.g., value vectors) of the vision encoder, while remaining a black-box to the LLM. This process utilizes only input images without labels, with the entire model architecture kept frozen. (b) We evaluate Doubly-UAP across various tasks. In this classification example, Cosine Similarity (CosSim) is used to measure top-k accuracy and attack success rates, comparing the model’s adversarial responses to either the ground truth label or original image embeddings generated by the CLIP text encoder.

related to the image, thereby achieving a doubly universal effect across both image and text inputs. Given that vision encoders are crucial for processing visual information, we aim to disrupt them to create effective perturbations. Previous research [4, 34, 40, 55] shows that altering the vision encoder’s output embeddings can effectively deceive the language model for specific images. However, it does not yield the desired results when we attempt to extend prior work to UAP generation. While attacks on a single image are successful, it poses significant challenges to create a UAP that universally deceives the LLM, utilizing the vision encoder alone. This observation highlights the need to explore a novel approach to address the complexity of generalizing a universal perturbation across image and text inputs.

To address these challenges, we propose **Doubly Universal Adversarial Perturbation (Doubly-UAP)**, the first UAP specifically designed for VLMs, as shown in Fig. 2. As a pioneering research, we focus on disrupting the core processes of the vision encoder by targeting the attention mechanism, which interprets visual features. Specifically, we analyze the two most critical components of this mechanism: the attention weights, which determine how each patch relates to others, and the value vectors, which carry the actual information within each patch. After identifying the most vulnerable components across layers—the value vectors in the middle-to-late layers—we target them to optimize the UAP, keeping the overall model architecture frozen. In particular, our label-free approach uses only input images to corrupt their original characteristics and visual properties. As a result, our Doubly-UAP is highly effective on VLMs across diverse image and text inputs, even though it is generated using only the vision encoder. This demonstrates that Doubly-UAP is able to deceive the lan-

guage model within the VLM as well, despite being updated in a black-box manner with respect to the LLM.

Our method is comprehensively evaluated across multiple tasks, including classification, captioning, and visual question answering (VQA). For classification and captioning, we use ImageNet [6] dataset, while VQA performance was assessed on five benchmarks: VQAv2 [12], ScienceQA [27], TextVQA [35], POPE [20], and MME [10]. The experimental results show that our approach consistently outperforms baseline methods across various image and text inputs, achieving state-of-the-art attack success rates. Additionally, we conduct extensive ablation studies and further analyzed how Doubly-UAP affects the attention mechanism. Our contributions are as follows:

- **First UAP for VLMs across Image and Text Inputs:** We introduce Doubly-UAP, the novel UAP specifically tailored for VLMs which is universal across both image and text inputs. Doubly-UAP is optimized in a label-free approach, with the entire model architecture frozen.
- **Black-Box Optimization for LLMs:** We optimize the Doubly-UAP by targeting only the vision encoder’s attention mechanism. Even when the LLM remains a black box, our approach successfully deceives the VLM.
- **Attention Mechanism Analysis:** We analyze the impact of each attention mechanism component within the vision encoder on the LLM, and further analyze how Doubly-UAP disrupts this mechanism.
- **Robust Performance Across Tasks:** Extensive evaluations across multiple tasks including classification, captioning, and VQA demonstrate that Doubly-UAP consistently outperforms baseline methods, achieving state-of-the-art (SOTA) attack success rates.

2. Related Work

2.1. Large Vision-Language Models

Large vision-language models (VLMs) [5, 24, 25] integrate visual information into large language models (LLMs) [3, 38] by using a vision encoder from vision-language pre-training models [33, 37]. This approach enables VLMs to process and understand both visual and textual data, enhancing their ability to generate responses that incorporate complex, multimodal inputs.

LLaVA [25] obtains the visual features with the pre-trained CLIP [33] vision encoder, and then puts them into the LLM along with the text prompt. LLaVA-1.5 [24] further improves its performance with simple modifications to LLaVA, and adding VQA data. InstructBLIP [5] utilizes the EVA-CLIP [37] vision encoder and Q-Former to obtain visual features.

2.2. Universal Adversarial Attacks

In the first stage, studies on adversarial attacks aim to generate image-specific adversarial perturbations [1, 7, 8, 11, 17, 21, 36, 48]. Afterward, Moosavi-Dezfooli et al. [29] show the existence of a universal adversarial perturbation (UAP), a single perturbation that can fool image classifiers when added to any input images. Since then, numerous studies have emerged on UAPs designed for deep learning models dealing with various tasks involving images or videos, such as image classification [13, 15, 18, 23, 29–31, 51, 52], object detection [2, 26, 39, 41, 46, 47, 53], and action recognition [9, 14, 16, 19, 42–45, 49, 50, 54]. However, no attempts have been made to generate UAPs for VLM models, despite the emergence of adversarial attacks on VLMs [4, 28, 32, 34, 40, 55].

2.3. Adversarial Attacks on Large Vision-Language Models

The field of adversarial attacks and jailbreaks on large vision-language models (VLMs) has recently gained attention. VLM attack methods can be categorized into two primary approaches: targeting vision encoders [4, 34, 40, 55] and targeting the large language models (LLMs) [28, 32].

Vision Encoder Attacks. Cui et al. [4] propose a method that reduces the cosine similarity between the image embedding of an adversarial image and its corresponding text embedding. Here, the image embedding is obtained from the VLM’s vision encoder (e.g., CLIP vision encoder), and the text embedding is derived from the corresponding text encoder (e.g., CLIP text encoder). Zhao et al. [56] and Shayegani et al. [34] suggest targeted attacks, where they increase the similarity between the target image and the adversarial image within the image embedding space. The embeddings are also extracted using the VLM’s vision encoder. Similarly, AnyAttack [55] performs a targeted at-

tack within the image embedding space, but adopts an extra generative model that takes the original image as input and generates an adversarial perturbation. Wang et al. (2024) [40] take a dual-embedding approach, simultaneously using both image and text embeddings. Specifically, they update the adversarial image by reducing the similarity between the original and adversarial image embeddings while also decreasing the similarity between the adversarial image embedding and its corresponding text embedding at the same time.

Large Language Model Attacks. Luo et al. [28] and Qi et al. [32] focus on attacking the LLM within a VLM by modifying the adversarial images to alter the LLM’s output responses. They employ loss functions that directly steer responses toward specific target words or sentences. Qi et al. [32] propose a universal attack, but their approach differs significantly from ours. Their attack method is universal across text prompts, where a single adversarial image can jailbreak multiple text prompts.

Unlike previous work, our method introduces the first UAP for VLMs that achieves **double-universality** across both image and text inputs, without utilizing the LLM.

3. Preliminary

3.1. Adversarial Attacks on Large Vision-Language Models (VLMs)

Adversarial attacks are techniques used to subtly modify input data in order to mislead machine learning models into producing incorrect predictions. In the context of Vision-Language Models (VLMs) that process both image and text inputs, these attacks introduce small, often imperceptible perturbations to the image data to manipulate the model’s output. Given an input image $x \in \mathcal{X}$, a label y , a text prompt $p \in \mathcal{P}$, and a VLM $f : \mathcal{X} \times \mathcal{P} \rightarrow \mathcal{Y}$ (where \mathcal{Y} is the set of possible labels), an adversarial attack seeks to generate a perturbation $\delta \in \mathbb{R}^d$ that causes the model to predict incorrectly. The conditions for a standard adversarial attack can be described as follows:

- **For labeled data:** The perturbation should lead to an incorrect prediction.

$$f(x + \delta, p) \neq y. \quad (1)$$

- **For unlabeled data:** The perturbation should change the model’s output.

$$f(x + \delta, p) \neq f(x, p). \quad (2)$$

To make sure the perturbations remain imperceptible, we constrain the perturbation by enforcing $\|\delta\|_\infty \leq \epsilon$, where ϵ is a small positive constant that limits the maximum pixel-level perturbation.

	Layer	Classification		ScienceQA	
		LLaVA-1.5	I-BLIP	LLaVA-1.5	I-BLIP
<i>Attention</i>	All	31.0	18.4	30.7	47.3
	Early	65.8	45.1	32.2	49.8
	Middle	88.3	67.5	33.9	49.5
	Late	29.7	20.4	29.3	46.9
<i>Value</i>	All	21.8	40.5	28.0	50.3
	Early	65.5	62.7	32.1	50.5
	Middle	93.6	93.7	98.2	54.9
	Late	36.2	66.4	29.1	52.5
<i>Both (A + V)</i>	Middle	91.6	87.9	33.6	53.4

Table 1. **Effectiveness of attention weights and value vectors.** The table shows the attack success rates (%) for attention weight and value vector attacks at each layer. The value vectors exhibit greater susceptibility compared to attention weights, while the impact of UAPs varies significantly across layers.

4. Analyzing the Impact of Vision Encoder’s Attention Mechanism on LLM

Our primary objective is to identify which specific components within the vision encoder’s attention mechanism most effectively influence the performance of the LLM. As a pioneering work in this area, we choose to focus on the two components with the most fundamental roles in the attention mechanism: (1) **Attention weights** control how much each patch should focus on other patches, determining the level of interaction or relevance between patches. We hypothesize that by targeting the attention weights, we can effectively interfere with the encoder’s ability to establish these relationships. (2) Meanwhile, **value vectors** hold the actual information within each patch. We expect that perturbing the value vectors will disrupt the essential information content within patches, further impairing the model’s interpretative abilities. Additionally, since the attention mechanism spans multiple layers, we explore whether their impact on LLM output varies across layers. For the experiment, we follow the ablation settings in Sec. 7.

4.1. Impact of Attention Weights and Value Vectors across Various Layers

To examine the influence of attention weights and value vectors on LLM performance, we first investigate each component individually across different layers in the vision encoder. We divide the vision encoder layers into three segments—early, middle, and late—along with an evaluation using all layers. Specifically, for the 24-layer CLIP vision encoder (for LLaVA-1.5), we group layers into sets of eight. Similarly, we divide the 39-layer EVA-CLIP vision encoder (for InstructBLIP) into sets of thirteen.

As shown in Tab. 1, the results reveal two primary observations. (1) **The impact of UAPs varies significantly across layers**, with the middle layers consistently demonstrating the highest vulnerability in both attention weights

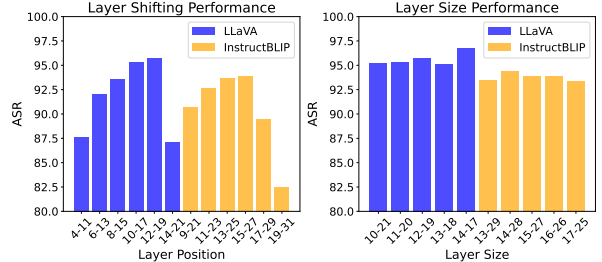


Figure 3. **Effectiveness across different layer configurations.** The left plot demonstrates the impact of varying the layer positions while keeping the window size constant. The right plot explores the effect of changing the number of layers while keeping the layer position fixed.

and value vectors. (2) **The value vectors exhibit greater susceptibility compared to attention weights**, suggesting that perturbations targeting the value vectors more significantly disrupt LLM responses. This trend is consistent across both the LLaVA-1.5 and InstructBLIP (I-BLIP) models, as well as across classification and VQA tasks, highlighting the pivotal role of value vectors in determining the LLM’s output.

4.2. Effect of Layer Shifting and Size Adjustments

Building on our earlier finding that the impact of UAPs varies significantly across layers, we further examine how layer selection influences attack performance by experimenting with layer shifting and size adjustments. Focusing on the most effective middle layers from the previous section, we shift the layer range and vary the number of layers within that range to identify optimal configurations.

The results in Fig. 3 illustrate the effects of shifting and adjusting the number of layers on the attack success rate. While the number of layers does not lead to substantial differences, both models show that middle-to-late layer ranges achieve the highest attack success rates. We adopt the layer ranges with the highest performance from these experiments as the main settings for our primary experiments.

5. Doubly-Universal Adversarial Perturbation (Doubly-UAP)

In this section, we propose **Doubly-UAP**, which is the first UAP specifically designed for VLMs. Our goal is to generate a UAP that distorts the visual information itself, thereby hindering the correct interpretation of images regardless of the text inputs, thereby achieving a doubly universal effect across both (1) **image** and (2) **text inputs**.

Formally, we define a Doubly-UAP as a perturbation δ that satisfies Eq. (1) and Eq. (2) for all images and text prompts $\forall x \in \mathcal{X}, \forall p \in \mathcal{P}$. As with standard adversarial attacks, we constrain Doubly-UAPs to be visually imperceptible by enforcing $\|\delta\|_\infty \leq \epsilon$, where ϵ is a small constant.

Vision-Language Model	Vision Encoder	Language Model
LLaVA [25]	CLIP ViT-L/14@224px [33]	Llama2-13B [38]
LLaVA-1.5 [24]	CLIP ViT-L/14@336px [33]	Vicuna-13B [3]
InstructBLIP [5]	EVA-CLIP [37]	Vicuna-13B [3]

Table 2. Vision encoders and language models used for each evaluated vision-language model.

To achieve this, we target the vision encoders within VLM, as it is crucial for visual interpretation. Specifically, we focus on the attention mechanism within the vision encoder, the core process responsible for interpreting visual features. We aim to disrupt this mechanism by targeting its most vulnerable components, the value vectors at the middle-to-late layers, based on the analysis from Sec. 4.

In detail, we maximize the loss between the original and adversarial value vectors extracted from these vulnerable layers. Let $V_l(x)$ represent value vectors associated with the l -th layer with input image x . Our objective is to find a perturbation δ^* that satisfies the following equation:

$$\delta^* = \arg \max_{\delta} \frac{1}{|L|} \sum_{l \in L} \text{Loss}(V_l(x), V_l(x + \delta)), \quad (3)$$

where $\text{Loss}(\cdot)$ is the loss function applied to the target vectors (discussed further in Sec. 7.1). Here, L denotes the set of layers used for the attack.

6. Experiments

6.1. Generation of UAP

6.1.1. Experiment Settings

To generate the Universal Adversarial Perturbations (UAPs), we select 200 images per class from the ImageNet [6] 2012 training dataset, resulting in a total of 200,000 images. The UAPs are optimized over three epochs with a batch size of 8, and the ϵ is set to $16/255$. The Adam optimizer with a learning rate of $1/255$ is used to update the UAPs. We extract value vectors from layers $L = \{14, \dots, 17\}$ for the CLIP vision encoder and layers $L = \{14, \dots, 28\}$ for the EVA-CLIP vision encoder. Cosine similarity loss is applied for $\text{Loss}(\cdot)$, as described in Sec. 7.1.

6.1.2. Models Utilized in Generation

We use three vision encoders as shown in Tab. 2 for UAP optimization: CLIP ViT-L/14@224px (CLIP-224) [33], CLIP ViT-L/14@336px (CLIP-336) [33], and EVA-CLIP [37] vision encoders. InstructBLIP uses the Q-Former with EVA-CLIP vision encoder for visual features, while we use EVA-CLIP vision encoder alone.

6.2. Evaluation of UAP

6.2.1. Tasks and Evaluation Metrics

We evaluate the UAPs on three tasks: (1) **classification**, (3) **image captioning**, and (3) **visual question answering**

Task	Text Prompt
Classification	“What is the main object in this image? Give an answer using a single word or phrase.”
Image Captioning	“What is this image about? Give an answer in a single sentence of about 10 words.”

Table 3. Text prompts used for classification and image captioning tasks, while Visual Question Answering (VQA) follows established benchmarks.

(VQA). For VQA, we follow established benchmarks as mentioned in Sec. 6.2.2. The evaluation is conducted using standard datasets and metrics widely accepted in VQA research. For both classification and image captioning tasks, we evaluate the Large Vision-Language Model (VLM) responses using the text prompts specified in Tab. 3. Following previous work [4], we base our evaluation on two primary metrics, as shown in Fig. 2-(b):

i. Attack Success Rate (ASR) (%): The CLIP text encoder is used to calculate the cosine similarity between clean and adversarial responses. If the similarity falls below a specified threshold, it is marked as a successful attack. We also denote **Sim(Avg.)**, which indicates the average cosine similarities between the original and the adversarial response embeddings.

ii. Top-k Accuracy (%): The CLIP text encoder is used to calculate cosine similarity between ground truth labels and adversarial responses. If the correct label is not among the top-k most similar outputs, the attack is considered successful. For captioning, clean response embeddings served as pseudo-ground truths.

6.2.2. Benchmarks and Datasets

For classification and image captioning, we select a total of 5,000 images by sampling five images from each class in the ImageNet [6] 2012 validation dataset. For VQA, we utilize five established benchmarks, including VQAv2 [12], ScienceQA [27], TextVQA [35], POPE [20], and MME [10]. VQAv2 utilizes COCO [22] 2015 test images, POPE utilizes COCO [22] 2014 validation images. ScienceQA, TextVQA, and MME each utilize their own unique datasets.

6.2.3. Models Utilized in Evaluation

For evaluation, we utilize three vision-language models listed in Tab. 2: LLaVA [25], LLaVA-1.5 [24], and InstructBLIP (I-BLIP) [5].

6.3. Baselines

As our method is the first to propose UAPs for VLMs, we extend existing image-specific VLM attack methods [4, 34, 40, 56] to a UAP framework, to establish three baselines. In each baseline, we aim to decrease the similarity between the adversarial image embeddings and their original counterparts. For image embeddings, we use the vision encoders within VLMs (e.g., CLIP vision encoder), while

		Classification (ImageNet)					Captioning (ImageNet)				
		ASR \uparrow (th=0.9)	ASR \uparrow (th=0.8)	Top-k \downarrow (k=1)	Top-k \downarrow (k=10)	Sim \downarrow (Avg.)	ASR \uparrow (th=0.7)	ASR \uparrow (th=0.6)	Top-k \downarrow (k=1)	Top-k \downarrow (k=10)	Sim \downarrow (Avg.)
LLaVA-1.5 (CLIP-336)	Clean	9.4	5.6	22.0	35.8	0.98	9.2	2.7	66.2	88.8	0.88
	Text-Emb [4]	29.9	20.7	18.2	31.6	0.93	46.6	31.2	30.7	54.2	0.70
	Img-Emb [34]	26.9	18.8	19.2	32.7	0.93	33.1	16.6	38.3	67.3	0.77
	Both-Emb [40]	24.8	16.9	19.6	33.2	0.94	30.1	15.5	42.7	71.1	0.78
	Doubly-UAP	96.1	92.5	1.0	2.5	0.72	95.3	83.3	1.7	3.5	0.48
LLaVA (CLIP-224)	Clean	22.1	10.5	26.0	45.3	0.94	7.6	1.8	65.4	90.4	0.86
	Text-Emb [4]	47.8	30.1	19.2	35.9	0.87	47.2	25.0	27.6	58.2	0.70
	Img-Emb [34]	67.9	52.8	12.5	24.1	0.78	74.9	56.7	13.1	30.8	0.58
	Both-Emb [40]	66.7	51.3	11.5	22.8	0.79	67.7	49.2	16.2	35.6	0.61
	Doubly-UAP	97.5	96.1	1.2	2.9	0.62	96.7	91.7	1.2	3.1	0.41
InstructBlip (EVA-CLIP)	Clean	3.5	2.3	26.0	39.3	0.99	6.9	2.1	82.6	96.4	0.89
	Text-Emb [4]	62.9	47.1	10.6	18.7	0.85	91.4	82.9	9.0	20.8	0.40
	Img-Emb [34]	23.3	15.9	22.8	36.2	0.94	42.9	23.2	45.6	76.4	0.72
	Both-Emb [40]	24.6	17.1	22.7	35.6	0.94	41.8	23.3	48.6	78.3	0.72
	Doubly-UAP	94.1	81.8	2.0	5.0	0.74	99.1	97.0	1.5	4.1	0.31

Table 4. Comparison of classification and captioning attack performance across UAP methods. Performance is evaluated using several metrics: **attack success rate (ASR, %)**, the percentage of cases with similarity below a threshold (th), with thresholds determined based on the Clean distribution in Fig. 4. **Top-K(%)** shows if the similarity ranks within the top k, and **Sim** shows the average similarity.

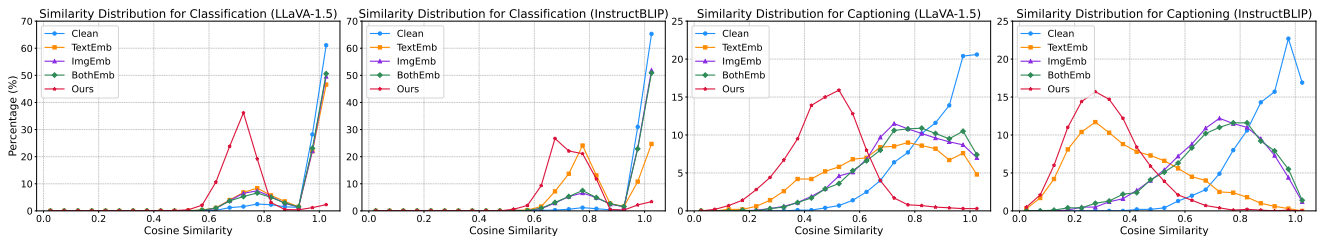


Figure 4. Cosine similarity distribution for classification and captioning. The **Clean** curves indicate high similarity between responses generated by original images compared with other responses from original images, while the **Ours** curves represent the lowest similarity when comparing responses generated by original images with those from adversarial images perturbed by the doubly-UAP attack.

corresponding text encoders (e.g., CLIP text encoder) are used for extracting text embeddings. The baselines are as follows:

i. Text Embedding Attack (Text-Emb) reduces cosine similarity between the ground truth text embedding (from “A photo of (class)”) and the adversarial image embedding, where (class) represents the ground truth ImageNet label. This baseline is the UAP-extended version of [4].

ii. Image Embedding Attack (Img-Emb) lowers cosine similarity between original and adversarial image embeddings from the VLM’s vision encoder. This baseline is the UAP-extended version of [34, 56].

iii. Both Embedding Attack (Both-Emb) simultaneously reduces cosine similarities for both (1) between the ground truth text embedding and the adversarial image embedding, and (2) between original and adversarial image embeddings. This baseline is the UAP-extended version of [40].

6.4. Main Results

6.4.1. Classification and Image Captioning

Table 4 shows the performance of Doubly-UAP compared to the baselines for classification and image captioning tasks. The results demonstrate that Doubly-UAP significantly outperforms baseline methods in both classification and image captioning tasks for all target VLMs, including LLaVA-1.5, LLaVA, and InstructBLIP. This is especially remarkable considering that the baseline Text-Emb directly utilizes the ground truth label of each image during UAP optimization, whereas Doubly-UAP is a label-free method.

For further analysis, we plot the cosine similarity distribution between original and adversarial responses for both the classification and the image captioning tasks on LLaVA-1.5 and InstructBLIP models, as shown in Fig. 4. It demonstrates that our Doubly-UAP induces the lowest cosine similarities between the clean and adversarial responses, indicating that the proposed method is the most effective among all evaluated methods for all target models.

		VQA (Score↓)						
		VQAv2	ScienceQA	TextVQA	POPE(rand)	POPE(pop)	POPE(adv)	MME
LLaVA-1.5 (CLIP-336)	Clean	80.0	73.4	61.3	88.1	87.5	85.6	1521.2
	Text-Emb [4]	69.6	69.4	54.1	86.2	84.9	80.6	1217.7
	Img-Emb [34]	72.1	71.8	55.4	84.4	81.5	80.1	1367.5
	Both-Emb [40]	74.7	70.0	56.2	86.2	80.3	79.8	1289.1
	Doubly-UAP	0.3	0.7	0.6	51.6	50.1	50.1	10.8
LLaVA (CLIP-336)	Clean	56.6	59.5	50.2	66.3	63.7	58.4	747.8
	Text-Emb [4]	43.8	55.0	44.8	56.2	53.0	51.8	635.9
	Img-Emb [34]	50.7	57.0	48.0	56.4	54.0	52.9	621.5
	Both-Emb [40]	52.8	58.0	47.4	58.9	55.8	53.2	699.0
	Doubly-UAP	2.1	1.7	2.9	52.0	50.5	50.3	23.6
InstructBlip (EVA-CLIP)	Clean	75.6	54.3	32.5	88.1	85.5	82.8	1236.7
	Text-Emb [4]	57.7	45.8	26.6	82.3	78.4	72.0	849.7
	Img-Emb [34]	69.9	50.6	30.1	86.2	83.5	79.7	1109.1
	Both-Emb [40]	70.4	49.0	29.6	86.4	83.5	80.1	1115.9
	Doubly-UAP	46.8	44.6	26.3	69.5	66.9	61.5	754.5

Table 5. Comparison of Visual Question Answering (VQA) performance across different models and UAP methods. The full score of the MME benchmark is 2000. Other benchmarks use accuracy (%) as their score. A lower score indicates a more successful attack.




	Classification: What is the main object in this image? Give an answer using a single word or phrase.
	Image Captioning: What is this image about? Give an answer in a single sentence of about 10 words.
	VQA (VQAv2): How many people are there? Answer the question using a single word or phrase.

Figure 5. Examples of original and adversarial responses with Doubly-UAP. The responses are obtained from LLaVA-1.5 and InstructBLIP models. **Org** denotes the responses with original images and **Adv** denotes the responses with adversarial images. Doubly-UAPs are applied to images to obtain adversarial responses.

6.4.2. Visual Question Answering

As noted by the LLaVA-1.5 [24], LLaVA with the Llama2 language model tends to respond in full sentences rather than providing single-word or short-phrase answers. Therefore, for VQA tasks, we evaluate UAPs on LLaVA with the Vicuna-13B language model and the CLIP-336 vision encoder. Since both LLaVA and LLaVA-1.5 use the same CLIP-336 vision encoder for this section, we also use the same Doubly-UAP for both models.

Table 5 shows the performance of Doubly-UAP compared to the baselines for VQA benchmarks. The results demonstrate that Doubly-UAP outperforms baseline methods in various VQA benchmarks for all target VLMs. As VQA tasks cover a wide range of visual understanding tasks such as optical character recognition (OCR), counting, color recognition, numerical calculation, and so on, the results indicate that our Doubly-UAP achieves robust attack performance across such diverse vision-language un-

derstanding tasks. Please note that we applied the same Doubly-UAP to both LLaVA and LLaVA-1.5, and it proved its effectiveness for both models. This indicates that the **Doubly-UAP can be effective across multiple VLMs** that share the same vision encoder.

Figure 5 presents examples of actual responses from LLaVA-1.5 and InstructBLIP. Remarkably, Doubly-UAP demonstrates overwhelming performance on both LLaVA and LLaVA-1.5 models, as it entirely disrupts not only their visual understanding but also their linguistic capabilities. As shown in the figure, the LLaVA-1.5 model repeats a meaningless phrase when attacked with Doubly-UAP. This phenomenon also occurs in the LLaVA model.

7. Ablation studies

For the ablation study, we aim to identify a more effective setting for Doubly-UAP. We conduct experiments using settings similar to those in the main experiments, with UAPs

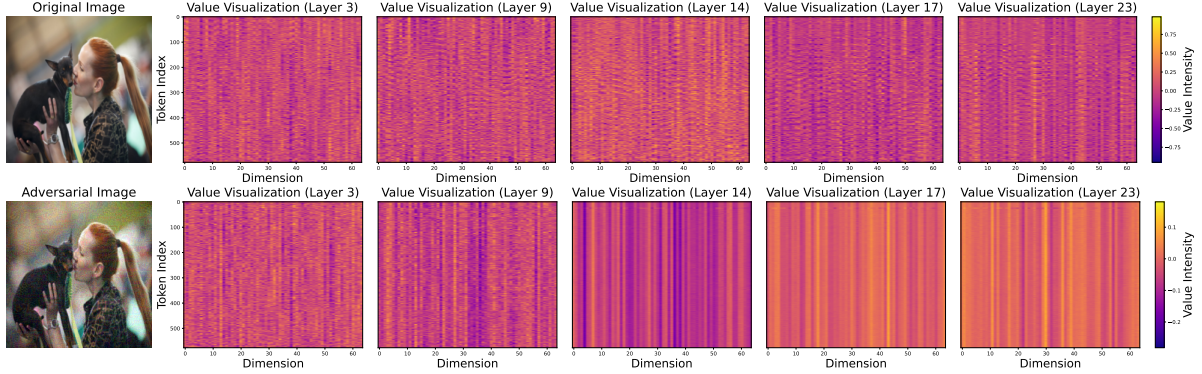


Figure 6. **Visualization of original and adversarial value vectors.** The upper row displays the original image and corresponding value vectors across layers. The lower row shows the adversarial image applied with Doubly-UAP and its corresponding value vectors. Adversarial value vectors exhibit significant distortion compared to the original value vectors, showing vertical stripe patterns.

Loss	Classification		ScienceQA	
	LLaVA-1.5	I-BLIP	LLaVA-1.5	I-BLIP
Std	70.1	77.9	45.7	50.8
MSE	93.8	85.4	33.8	53.8
CosSim	93.6	93.7	98.2	54.9

Table 6. Effectiveness of different loss functions.

updated for five epochs. For classification tasks, we select one image per class from the ImageNet validation dataset, totaling 1,000 images. Additional experiments, which could not be included here due to space constraints, are provided in the supplementary material.

7.1. Effectiveness of Different Loss Functions

The results in Tab. 6 show the attack success rates for each loss function applied during UAP generation: standard deviation (Std), Mean Squared Error (MSE), and cosine similarity (CosSim). The results reveal that cosine similarity loss consistently performs the best across both classification and VQA tasks, with the highest attack success rates observed for both LLaVA-1.5 and InstructBLIP models.

7.2. Ablation on Epsilon

Figure 7 shows the attack success rates of Doubly-UAP with diverse ϵ values. Doubly-UAP shows higher attack success rates with higher ϵ values. We select $\epsilon = 16/255$ as it yields the highest attack success rates.

8. Analysis of Value Vector Disruption

Figure 6 shows a comparison of value vector distributions before and after applying the Doubly-UAP, targeting layers 14-17 from the CLIP-336 vision encoder. The vertical axis represents token indexes, and the horizontal axis represents value vector dimensions across several layers.

Comparing the original and adversarial images, we observe clear distortions in the value vectors after applying

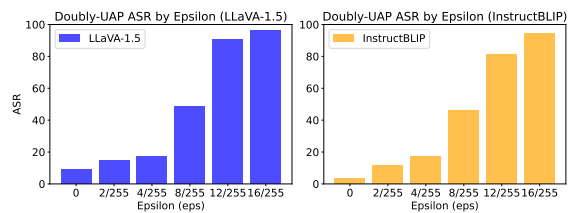


Figure 7. ASRs (%) of Doubly-UAPs at various epsilon values.

Doubly-UAP. In the adversarial patterns, vertical stripes emerge, indicating that each token has become increasingly similar. This suggests that the value vectors have lost their ability to properly capture distinct visual information from the image. Notably, this disruption not only affects the attack-targeted layers (14-17) but also propagates to non-target layers, such as layer 23, and even earlier layers like layer 9. These patterns indicate that the perturbation could impact the model’s internal structure across multiple layers, ultimately hindering its ability to interpret semantic information from the image.

9. Conclusion

In this paper, we introduced Doubly Universal Adversarial Perturbation (Doubly-UAP), the first UAP specifically designed for VLMs, achieving universal effectiveness across diverse image and text inputs. Our method centers on disrupting the vision encoder’s attention mechanism, operating as a black-box attack for the LLM in a label-free manner. Extensive evaluations across tasks such as classification, captioning, and VQA demonstrated that Doubly-UAP consistently outperforms baseline methods, achieving high attack success rates and robustness. We further analyzed how the perturbation affects the attention mechanism, revealing its strong influence on VLM performance. This work highlights the importance of strengthening multimodal models against adversarial perturbations, laying the groundwork for future research focused on universal threats to VLMs.

References

- [1] Junyoung Byun, Seungju Cho, Myung-Joon Kwon, Hee-Seon Kim, and Changick Kim. Improving the transferability of targeted adversarial examples through object-based diverse input. In *Proceedings of the IEEE/CVF Conference on Computer Vision and Pattern Recognition*, pages 15244–15253, 2022. 3
- [2] Shang-Tse Chen, Cory Cornelius, Jason Martin, and Duen Horng Polo Chau. Shapeshifter: Robust physical adversarial attack on faster r-cnn object detector. In *Joint European Conference on Machine Learning and Knowledge Discovery in Databases*, pages 52–68. Springer, 2018. 3
- [3] Wei-Lin Chiang, Zhuohan Li, Zi Lin, Ying Sheng, Zhanghao Wu, Hao Zhang, Lianmin Zheng, Siyuan Zhuang, Yonghao Zhuang, Joseph E Gonzalez, et al. Vicuna: An open-source chatbot impressing gpt-4 with 90%* chatgpt quality. See <https://vicuna.lmsys.org> (accessed 14 April 2023), 2(3):6, 2023. 1, 3, 5
- [4] Xuanming Cui, Alejandro Aparcedo, Young Kyun Jang, and Ser-Nam Lim. On the robustness of large multimodal models against image adversarial attacks. In *Proceedings of the IEEE/CVF Conference on Computer Vision and Pattern Recognition*, pages 24625–24634, 2024. 1, 2, 3, 5, 6, 7
- [5] Wenliang Dai, Junnan Li, Dongxu Li, Anthony Tiong, Junqi Zhao, Weisheng Wang, Boyang Li, Pascale Fung, and Steven Hoi. Instructblip: Towards general-purpose vision-language models with instruction tuning. In *Thirty-seventh Conference on Neural Information Processing Systems*, 2023. 1, 3, 5
- [6] Jia Deng, Wei Dong, Richard Socher, Li-Jia Li, Kai Li, and Li Fei-Fei. Imagenet: A large-scale hierarchical image database. In *2009 IEEE conference on computer vision and pattern recognition*, pages 248–255. Ieee, 2009. 2, 5
- [7] Yinpeng Dong, Fangzhou Liao, Tianyu Pang, Hang Su, Jun Zhu, Xiaolin Hu, and Jianguo Li. Boosting adversarial attacks with momentum. In *Proceedings of the IEEE conference on computer vision and pattern recognition*, pages 9185–9193, 2018. 1, 3
- [8] Yinpeng Dong, Tianyu Pang, Hang Su, and Jun Zhu. Evading defenses to transferable adversarial examples by translation-invariant attacks. In *Proceedings of the IEEE/CVF Conference on Computer Vision and Pattern Recognition*, pages 4312–4321, 2019. 1, 3
- [9] Zhenyu Du, Fangzheng Liu, and Xuehu Yan. Sparse adversarial video attacks via superpixel-based jacobian computation. *Sensors*, 22(10):3686, 2022. 3
- [10] Chaoyou Fu, Peixian Chen, Yunhang Shen, Yulei Qin, Mengdan Zhang, Xu Lin, Jinrui Yang, Xiawu Zheng, Ke Li, Xing Sun, et al. Mme: A comprehensive evaluation benchmark for multimodal large language models. *arXiv preprint arXiv:2306.13394*, 2023. 2, 5
- [11] Ian Goodfellow, Jonathon Shlens, and Christian Szegedy. Explaining and harnessing adversarial examples. In *ICLR*, 2015. 1, 3
- [12] Yash Goyal, Tejas Khot, Douglas Summers-Stay, Dhruv Batra, and Devi Parikh. Making the v in vqa matter: Elevating the role of image understanding in visual question answering. In *Proceedings of the IEEE conference on computer vision and pattern recognition*, pages 6904–6913, 2017. 1, 2, 5, 6
- [13] Jamie Hayes and George Danezis. Learning universal adversarial perturbations with generative models. In *2018 IEEE Security and Privacy Workshops (SPW)*, pages 43–49. IEEE, 2018. 1, 3
- [14] Linxi Jiang, Xingjun Ma, Shaoxiang Chen, James Bailey, and Yu-Gang Jiang. Black-box adversarial attacks on video recognition models. In *Proceedings of the 27th ACM International Conference on Multimedia*, pages 864–872, 2019. 3
- [15] Valentin Khruikov and Ivan Oseledets. Art of singular vectors and universal adversarial perturbations. In *Proceedings of the IEEE Conference on Computer Vision and Pattern Recognition*, pages 8562–8570, 2018. 1, 3
- [16] Hee-Seon Kim, Minji Son, Minbeom Kim, Myung-Joon Kwon, and Changick Kim. Breaking temporal consistency: Generating video universal adversarial perturbations using image models. In *Proceedings of the IEEE/CVF International Conference on Computer Vision*, pages 4325–4334, 2023. 3
- [17] Alexey Kurakin, Ian J Goodfellow, and Samy Bengio. Adversarial examples in the physical world. In *5th International Conference on Learning Representations, ICLR, Workshop Track Proceedings*, 2017. 1, 3
- [18] Maosen Li, Yanhua Yang, Kun Wei, Xu Yang, and Heng Huang. Learning universal adversarial perturbation by adversarial example. In *Proceedings of the AAAI Conference on Artificial Intelligence*, pages 1350–1358, 2022. 1, 3
- [19] Shasha Li, Abhishek Aich, Shitong Zhu, Salman Asif, Chengyu Song, Amit Roy-Chowdhury, and Srikanth Krishnamurthy. Adversarial attacks on black box video classifiers: Leveraging the power of geometric transformations. *Advances in Neural Information Processing Systems*, 34:2085–2096, 2021. 3
- [20] Yifan Li, Yifan Du, Kun Zhou, Jinpeng Wang, Wayne Xin Zhao, and Ji-Rong Wen. Evaluating object hallucination in large vision-language models. *arXiv preprint arXiv:2305.10355*, 2023. 2, 5, 1, 7
- [21] Jiadong Lin, Chuanbiao Song, Kun He, Liwei Wang, and John E Hopcroft. Nesterov accelerated gradient and scale invariance for adversarial attacks. In *International Conference on Learning Representations*, 2020. 1, 3
- [22] Tsung-Yi Lin, Michael Maire, Serge Belongie, James Hays, Pietro Perona, Deva Ramanan, Piotr Dollár, and C Lawrence Zitnick. Microsoft coco: Common objects in context. In *European conference on computer vision*, pages 740–755. Springer, 2014. 5
- [23] Hong Liu, Rongrong Ji, Jie Li, Baochang Zhang, Yue Gao, Yongjian Wu, and Feiyue Huang. Universal adversarial perturbation via prior driven uncertainty approximation. In *Proceedings of the IEEE/CVF International Conference on Computer Vision*, pages 2941–2949, 2019. 1, 3
- [24] Haotian Liu, Chunyuan Li, Yuheng Li, and Yong Jae Lee. Improved baselines with visual instruction tuning. In *Proceedings of the IEEE/CVF Conference on Computer Vision and Pattern Recognition*, pages 26296–26306, 2024. 1, 3, 5, 7

- [25] Haotian Liu, Chunyuan Li, Qingyang Wu, and Yong Jae Lee. Visual instruction tuning. *Advances in neural information processing systems*, 36, 2024. 1, 3, 5
- [26] Xin Liu, Huanrui Yang, Ziwei Liu, Linghao Song, Hai Li, and Yiran Chen. Dpatch: An adversarial patch attack on object detectors. *arXiv preprint arXiv:1806.02299*, 2018. 3
- [27] Pan Lu, Swaroop Mishra, Tony Xia, Liang Qiu, Kai-Wei Chang, Song-Chun Zhu, Oyvind Tafjord, Peter Clark, and Ashwin Kalyan. Learn to explain: Multimodal reasoning via thought chains for science question answering. In *The 36th Conference on Neural Information Processing Systems (NeurIPS)*, 2022. 1, 2, 5, 6
- [28] Haochen Luo, Jindong Gu, Fengyuan Liu, and Philip Torr. An image is worth 1000 lies: Adversarial transferability across prompts on vision-language models. *arXiv preprint arXiv:2403.09766*, 2024. 1, 3
- [29] Seyed-Mohsen Moosavi-Dezfooli, Alhussein Fawzi, Omar Fawzi, and Pascal Frossard. Universal adversarial perturbations. In *Proceedings of the IEEE conference on computer vision and pattern recognition*, pages 1765–1773, 2017. 1, 3
- [30] KR Mopuri, U Garg, and R Venkatesh Babu. Fast feature fool: A data independent approach to universal adversarial perturbations. In *British Machine Vision Conference 2017, BMVC 2017*. BMVA Press, 2017.
- [31] Konda Reddy Mopuri, Aditya Ganeshan, and R Venkatesh Babu. Generalizable data-free objective for crafting universal adversarial perturbations. *IEEE transactions on pattern analysis and machine intelligence*, 41(10):2452–2465, 2018. 1, 3
- [32] Xiangyu Qi, Kaixuan Huang, Ashwinee Panda, Peter Henderson, Mengdi Wang, and Prateek Mittal. Visual adversarial examples jailbreak aligned large language models. In *Proceedings of the AAAI Conference on Artificial Intelligence*, pages 21527–21536, 2024. 1, 3
- [33] Alec Radford, Jong Wook Kim, Chris Hallacy, Aditya Ramesh, Gabriel Goh, Sandhini Agarwal, Girish Sastry, Amanda Askell, Pamela Mishkin, Jack Clark, et al. Learning transferable visual models from natural language supervision. In *International conference on machine learning*, pages 8748–8763. PMLR, 2021. 1, 3, 5
- [34] Erfan Shayegani, Yue Dong, and Nael Abu-Ghazaleh. Jailbreak in pieces: Compositional adversarial attacks on multimodal language models. In *The Twelfth International Conference on Learning Representations*, 2023. 1, 2, 3, 5, 6, 7
- [35] Amanpreet Singh, Vivek Natarajan, Meet Shah, Yu Jiang, Xinlei Chen, Dhruv Batra, Devi Parikh, and Marcus Rohrbach. Towards vqa models that can read. In *Proceedings of the IEEE/CVF conference on computer vision and pattern recognition*, pages 8317–8326, 2019. 1, 2, 5, 7
- [36] Minji Son, Myung-Joon Kwon, Hee-Seon Kim, Junyoung Byun, Seungju Cho, and Changick Kim. Adaptive warping network for transferable adversarial attacks. In *2022 IEEE International Conference on Image Processing (ICIP)*, pages 3056–3060. IEEE, 2022. 3
- [37] Quan Sun, Yuxin Fang, Ledell Wu, Xinlong Wang, and Yue Cao. Eva-clip: Improved training techniques for clip at scale. *arXiv preprint arXiv:2303.15389*, 2023. 1, 3, 5
- [38] Hugo Touvron, Louis Martin, Kevin Stone, Peter Albert, Amjad Almahairi, Yasmine Babaei, Nikolay Bashlykov, Soumya Batra, Prajjwal Bhargava, Shruti Bhosale, et al. Llama 2: Open foundation and fine-tuned chat models. *arXiv preprint arXiv:2307.09288*, 2023. 1, 3, 5
- [39] Yajie Wang, Yu-an Tan, Wenjiao Zhang, Yuhang Zhao, and Xiaohui Kuang. An adversarial attack on dnn-based black-box object detectors. *Journal of Network and Computer Applications*, 161:102634, 2020. 3
- [40] Yubo Wang, Chaohu Liu, Yanqiu Qu, Haoyu Cao, Deqiang Jiang, and Linli Xu. Break the visual perception: Adversarial attacks targeting encoded visual tokens of large vision-language models. *arXiv preprint arXiv:2410.06699*, 2024. 1, 2, 3, 5, 6, 7
- [41] Xingxing Wei, Siyuan Liang, Ning Chen, and Xiaochun Cao. Transferable adversarial attacks for image and video object detection. In *Proceedings of the Twenty-Eighth International Joint Conference on Artificial Intelligence*. International Joint Conferences on Artificial Intelligence Organization, 2019. 3
- [42] Zhipeng Wei, Jingjing Chen, Xingxing Wei, Linxi Jiang, Tat-Seng Chua, Fengfeng Zhou, and Yu-Gang Jiang. Heuristic black-box adversarial attacks on video recognition models. In *Proceedings of the AAAI Conference on Artificial Intelligence*, pages 12338–12345, 2020. 3
- [43] Zhipeng Wei, Jingjing Chen, Zuxuan Wu, and Yu-Gang Jiang. Cross-modal transferable adversarial attacks from images to videos. In *Proceedings of the IEEE/CVF conference on computer vision and pattern recognition*, pages 15064–15073, 2022.
- [44] Zhipeng Wei, Jingjing Chen, Zuxuan Wu, and Yu-Gang Jiang. Boosting the transferability of video adversarial examples via temporal translation. In *Proceedings of the AAAI Conference on Artificial Intelligence*, pages 2659–2667, 2022.
- [45] Zhipeng Wei, Jingjing Chen, Hao Zhang, Linxi Jiang, and Yu-Gang Jiang. Adaptive temporal grouping for black-box adversarial attacks on videos. In *Proceedings of the 2022 International Conference on Multimedia Retrieval*, pages 587–593, 2022. 3
- [46] Zuxuan Wu, Ser-Nam Lim, Larry S Davis, and Tom Goldstein. Making an invisibility cloak: Real world adversarial attacks on object detectors. In *European Conference on Computer Vision*, pages 1–17. Springer, 2020. 3
- [47] Cihang Xie, Jianyu Wang, Zhishuai Zhang, Yuyin Zhou, Lingxi Xie, and Alan Yuille. Adversarial examples for semantic segmentation and object detection. In *Proceedings of the IEEE international conference on computer vision*, pages 1369–1378, 2017. 3
- [48] Cihang Xie, Zhishuai Zhang, Yuyin Zhou, Song Bai, Jianyu Wang, Zhou Ren, and Alan L Yuille. Improving transferability of adversarial examples with input diversity. In *Proceedings of the IEEE/CVF Conference on Computer Vision and Pattern Recognition*, pages 2730–2739, 2019. 1, 3
- [49] Shangyu Xie, Han Wang, Yu Kong, and Yuan Hong. Universal 3-dimensional perturbations for black-box attacks on video recognition systems. In *2022 IEEE Symposium on Security and Privacy (SP)*, pages 1390–1407. IEEE, 2022. 3

- [50] Yixiao Xu, Xiaolei Liu, Mingyong Yin, Teng Hu, and Kangyi Ding. Sparse adversarial attack for video via gradient-based keyframe selection. In *ICASSP 2022-2022 IEEE International Conference on Acoustics, Speech and Signal Processing (ICASSP)*, pages 2874–2878. IEEE, 2022. [3](#)
- [51] Chaoning Zhang, Philipp Benz, Tooba Imtiaz, and In-So Kweon. Cd-uap: Class discriminative universal adversarial perturbation. In *Proceedings of the AAAI conference on artificial intelligence*, pages 6754–6761, 2020. [1](#), [3](#)
- [52] Chaoning Zhang, Philipp Benz, Adil Karjauv, and In So Kweon. Data-free universal adversarial perturbation and black-box attack. In *Proceedings of the IEEE/CVF International Conference on Computer Vision*, pages 7868–7877, 2021. [1](#), [3](#)
- [53] Hantao Zhang, Wengang Zhou, and Houqiang Li. Contextual adversarial attacks for object detection. In *2020 IEEE International Conference on Multimedia and Expo (ICME)*, pages 1–6. IEEE, 2020. [3](#)
- [54] Hu Zhang, Linchao Zhu, Yi Zhu, and Yi Yang. Motion-excited sampler: Video adversarial attack with sparked prior. In *Computer Vision–ECCV 2020: 16th European Conference, Glasgow, UK, August 23–28, 2020, Proceedings, Part XX 16*, pages 240–256. Springer, 2020. [3](#)
- [55] Jiaming Zhang, Junhong Ye, Xingjun Ma, Yige Li, Yunfan Yang, Jitao Sang, and Dit-Yan Yeung. Anyattack: Towards large-scale self-supervised generation of targeted adversarial examples for vision-language models. *arXiv preprint arXiv:2410.05346*, 2024. [1](#), [2](#), [3](#)
- [56] Yunqing Zhao, Tianyu Pang, Chao Du, Xiao Yang, Chongxuan Li, Ngai-Man Man Cheung, and Min Lin. On evaluating adversarial robustness of large vision-language models. *Advances in Neural Information Processing Systems*, 36, 2024. [3](#), [5](#), [6](#)

Doubly-Universal Adversarial Perturbations: Deceiving Vision-Language Models Across Both Images and Text with a Single Perturbation

Supplementary Material

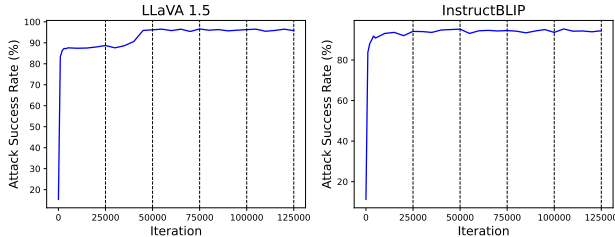


Figure 8. **Ablation on update iterations.** This plot shows the attack success rates (%) of the UAP over iterations. Each vertical line represents the end of an epoch. The UAPs are optimized with the CLIP-336 and EVA-CLIP vision encoder and evaluated on the LLaVA-1.5 and the InstructBLIP models, respectively.

10. Ablation on Update Iterations

In this section, we conduct an ablation study on update iterations. The results are presented in Fig. 8. The UAP achieves the highest attack success rate at the third epoch for LLaVA-1.5 [24] and at the second for the InstructBLIP [5]. As attack success rates converge sufficiently at the third epoch, we update the UAPs for three epochs for the main experiments.

11. Doubly-UAP Visualization

Figure 9 visualizes the Doubly-UAPs generated using three vision encoders: CLIP-224 [33], CLIP-336 [33], and EVA-CLIP [37]. The patterns highlight distinct characteristics of the perturbations derived from each model.

12. Model Responses Under Doubly-UAP Attacks

In this section, we report the responses of LLaVA-1.5 [24] and InstructBLIP [5] models with original and adversarial images for classification, image captioning, and visual question answering (VQA) tasks. Figure 10 shows the responses for the classification task, Figs. 11 and 12 show the responses for the image captioning task, and Figs. 13 and 14 show the responses for various VQA benchmarks including VQAv2 [12], ScienceQA [27], TextVQA [35], and POPE [20] benchmarks. We apply our Doubly-UAPs to the images to obtain the adversarial images.

As shown in these figures, our Doubly-UAP significantly disrupts both the linguistic and visual understanding capabilities of the LLaVA-1.5 model, regardless of

the input images or text prompts. Attacked with Doubly-UAP LLaVA-1.5 model respond with repeating meaningless words, across classification, image captioning, and VQA tasks.

In contrast, the InstructBLIP model retains its ability to understand text prompts and respond in an appropriate format, even under the influence of Doubly-UAP attacks. However, the severe degradation of the visual representation prevents accurate image interpretation, resulting in responses that diverge significantly from the correct answers, across classification, image captioning, and VQA tasks.

These results demonstrate that our Doubly-UAP is highly effective in disrupting the visual representations of images, achieving a doubly-universal adversarial effect on both images and text inputs.

13. Supplementary Analysis of Value Vector Disruption

To provide further insights into the impact of Doubly-UAP on value vector, we offer additional visualizations for both CLIP-336 [33] and EVA-CLIP [37] vision encoders. Figures 15 and 16 compares value vector distributions before and after applying the Doubly-UAP, targeting layers 14-17 in the CLIP-336 vision encoder and layers 14-28 in the EVA-CLIP vision encoder, as in the main paper. The vertical axis represents token indexes, and the horizontal axis represents value vector dimensions across several layers.

As shown in Fig. 15, the value vector distributions of the CLIP-336 vision encoder exhibit significant distortions after applying Doubly-UAP. Targeted layers (14-17) show clear vertical stripe patterns, indicating high similarity between token embeddings. This disruption propagates to earlier layers, such as layer 9, and later layers, such as layer 23, demonstrating that the perturbation propagates throughout the layers. Across all images, this consistent disruption underscores the effectiveness of Doubly-UAP in degrading the distribution of value vectors and impairing the encoder’s visual representation capabilities.

As shown in Fig. 16, the effect of Doubly-UAP on the EVA-CLIP vision encoder also reveals a clear disruption in the value vector distributions, with a noticeable loss of distinctive visual patterns in the targeted layers (14-28). The value vectors in these layers become partially uniform, diminishing their ability to encode meaningful, image-specific features. This disruption is not limited to the targeted layers but extends to earlier layers, such as layer 3, and later layers, such as layer 38. The partial uniformity and

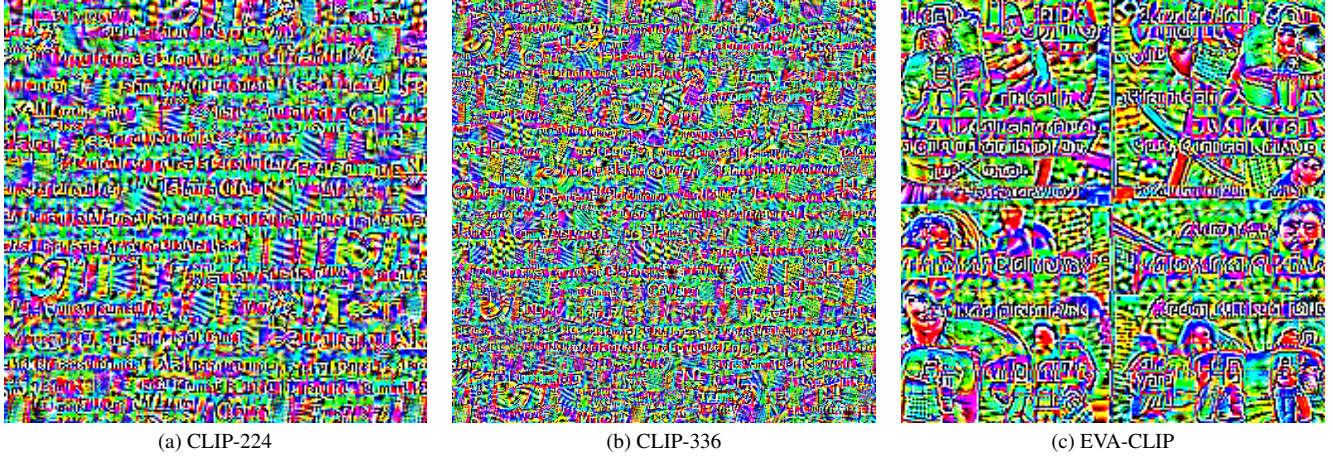


Figure 9. Visualization of Doubly-UAP perturbations from various vision encoders.

degradation observed in the adversarial value vectors underscore the strength of Doubly-UAP in impairing the vision encoder’s ability to effectively capture and preserve critical visual representations.

Also, in both CLIP and EVA-CLIP, it is observed that after applying doubly-UAP, the value distributions become similar regardless of the input image. For example, in layer 23 of the CLIP vision encoder, the vertical stripe patterns appear consistent across different input images, with the positions of bright and dark areas remaining unchanged. Similarly, in layer 14 of the EVA-CLIP vision encoder, the value patterns remain similar despite variations in the input image.


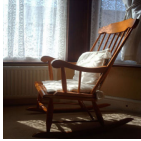



Captioning Prompt: What is this image about?\nGive an answer in a single sentence of about 10 words.	
	<p>LLaVA-1.5 Org: A person is flying in the sky with a parachute.</p> <p>→ Adv: the company.\n the image.\n the image.\n the image of the image of the image.\n the context of the image.\n the image of the image of the image of the image of the image of the image of the image of</p>
	<p>InstructBLIP Org: A man is skydiving with a red and black parachute in the sky.</p> <p>→ Adv: This image showcases a collection of colorful stickers featuring different animals, including elephants, giraffes, lions, and tigers.</p>
	<p>LLaVA-1.5 Org: A wooden rocking chair with a white pillow on it.</p> <p>→ Adv: the ess the importance of the context.\n the context.\n the context of the situation.\n the context of the context of the situation of the context of the esses the context of the context of the context of the context of the context</p>
	<p>InstructBLIP Org: A rocking chair is placed in front of a window, with sunlight shining through the curtains and illuminating the room.</p> <p>→ Adv: This image is a collection of posters showcasing various artworks, including paintings, sculptures, and other forms of visual art.</p>
	<p>LLaVA-1.5 Org: A green vase with flowers in it.</p> <p>→ Adv: the context of the situation.\n the context of the situation.\n the context of the situation of the context of the situation of the context of the situation.\n the context of the situation of the context of the situation of the context of the context</p>
	<p>InstructBLIP Org: A green vase filled with colorful flowers sits on top of a dining table, surrounded by various cups and saucers.</p> <p>→ Adv: A collage of images showcasing a variety of products and services offered by a hair salon, including haircuts, styling, coloring, and more</p>
	<p>LLaVA-1.5 Org: A red panda is laying on a rock.</p> <p>→ Adv: the image of a picture of the image of the picture.</p>
	<p>InstructBLIP Org: A red panda is standing on a rocky surface, looking towards the left side of the image.</p> <p>→ Adv: This image showcases a collage of colorful images, depicting people in various poses and settings.</p>
	<p>LLaVA-1.5 Org: A white game controller with a red button.</p> <p>→ Adv: The image is a single sentence of 100000000 words.</p>
	<p>InstructBLIP Org: A Nintendo Entertainment System (NES) controller is placed on a carpeted surface.</p> <p>→ Adv: A collage of various images, including a pair of scissors and a calculator, is displayed in this image.</p>

Figure 11. **Responses with original and adversarial images for image captioning task (Part 1).** The figure shows the responses of LLaVA-1.5 and InstructBLIP models with original and adversarial images for the image captioning task. **Org** denotes responses with original images and **Adv** denotes responses with adversarial images. Doubly-UAPs are applied to images to obtain adversarial images.

Captioning Prompt: What is this image about?\nGive an answer in a single sentence of about 10 words.






	LLaVA-1.5	Org: A small bird perched on a tree branch. → Adv: the image.\nthe image of the scene. the image.\nthe image of the image.\nthe image of the image of the image of the image of the image of the image of the image of the image
	InstructBLIP	Org: A small bird is perched on a thin tree branch, looking towards the camera. → Adv: This image is a collection of advertisements or promotional materials, showcasing various products and services. The advertisements are displayed in a collage format, with each one featuring a different product or service. Some of the advertisements feature people, while others showcase animals, such as elephants. The advertisements are colorful and eye-catching, designed to attract the attention of potential customers.
	LLaVA-1.5	Org: A dog with a purple collar is running in the grass. → Adv: the context of the situation.\nthe context of the context of the situation.\nthe context of the situation of the context of the situation of the context of the situation of the context
	InstructBLIP	Org: A dog is running on a field, wearing a harness. → Adv: This image is a collection of advertisements for various products and services.
	LLaVA-1.5	Org: Two goats on a rocky hill. → Adv: the importance of the situation. the different.\nthe context of the image of the situation.\nthe context of the situation of the situation of the situation of the context of the situation of the situation of the context of the situation of the context of
	InstructBLIP	Org: Two goats are standing on top of a rocky cliff, enjoying the scenic view. → Adv: This image is a collage of four posters, each showcasing a different artistic representation of a woman carrying a backpack. The posters appear to be advertisements for an outdoor adventure or camping trip.
	LLaVA-1.5	Org: A pen is on a piece of paper. → Adv: the context of the situation.
	InstructBLIP	Org: A pen is placed on top of a notebook, with several lines of handwritten text visible in the background. → Adv: A collage of images featuring people in various poses is displayed on a wall.
	LLaVA-1.5	Org: A large green machine is plowing a field. → Adv: the image of the image of the image.\nthe image of the image of the image of the image of the image of the image of the picture of the image of the image of the image of the image of the image of the image of the image of the image of
	InstructBLIP	Org: A combine harvester is working in a wheat field. → Adv: This image showcases a collection of advertisements for an art exhibit, featuring various paintings and drawings depicting different scenes and characters.

Figure 12. **Responses with original and adversarial images for image captioning task (Part 2).** The figure shows responses of LLaVA-1.5 and InstructBLIP models with original and adversarial images for the image captioning task. **Org** denotes responses with original images and **Adv** denotes responses with adversarial images. Doubly-UAPs are applied to images to obtain adversarial images.

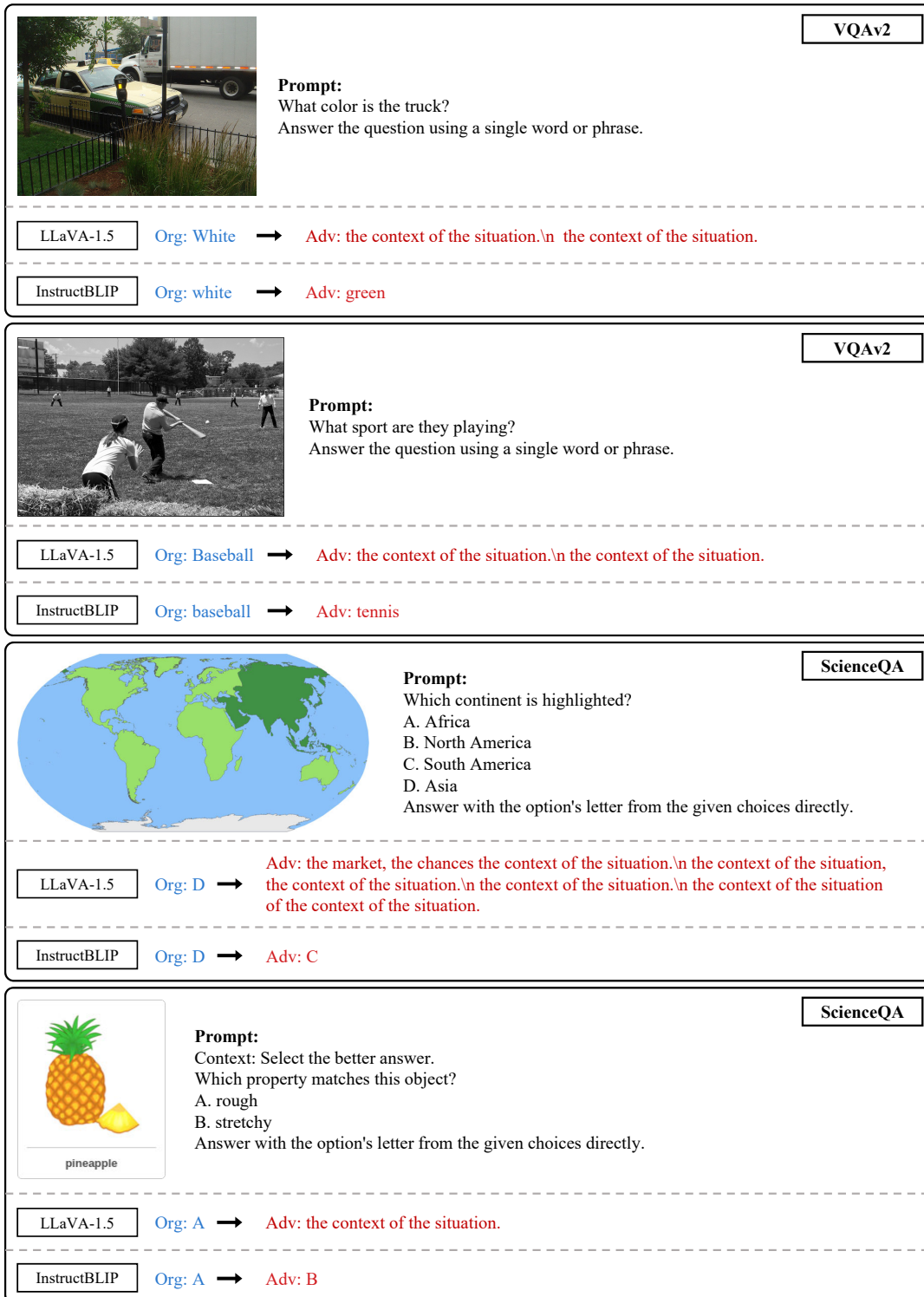


Figure 13. **Responses with original and adversarial images for VQA benchmarks (Part 1).** The figure shows responses of LLaVA-1.5 and InstructBLIP models with original and adversarial images for VQA_{v2} [12] and ScienceQA [27] benchmarks. **Org** denotes responses with original images and **Adv** denotes responses with adversarial images. Doubly-UAPs are applied to images to obtain adversarial images.



Figure 14. Responses with original and adversarial images for VQA benchmarks (Part 2). The figure shows responses of LLaVA-1.5 and InstructBLIP models with original and adversarial images for TextVQA [35] and POPE [20] benchmarks. **Org** denotes responses with original images and **Adv** denotes responses with adversarial images. Doubly-UAPs are applied to images to obtain adversarial images.

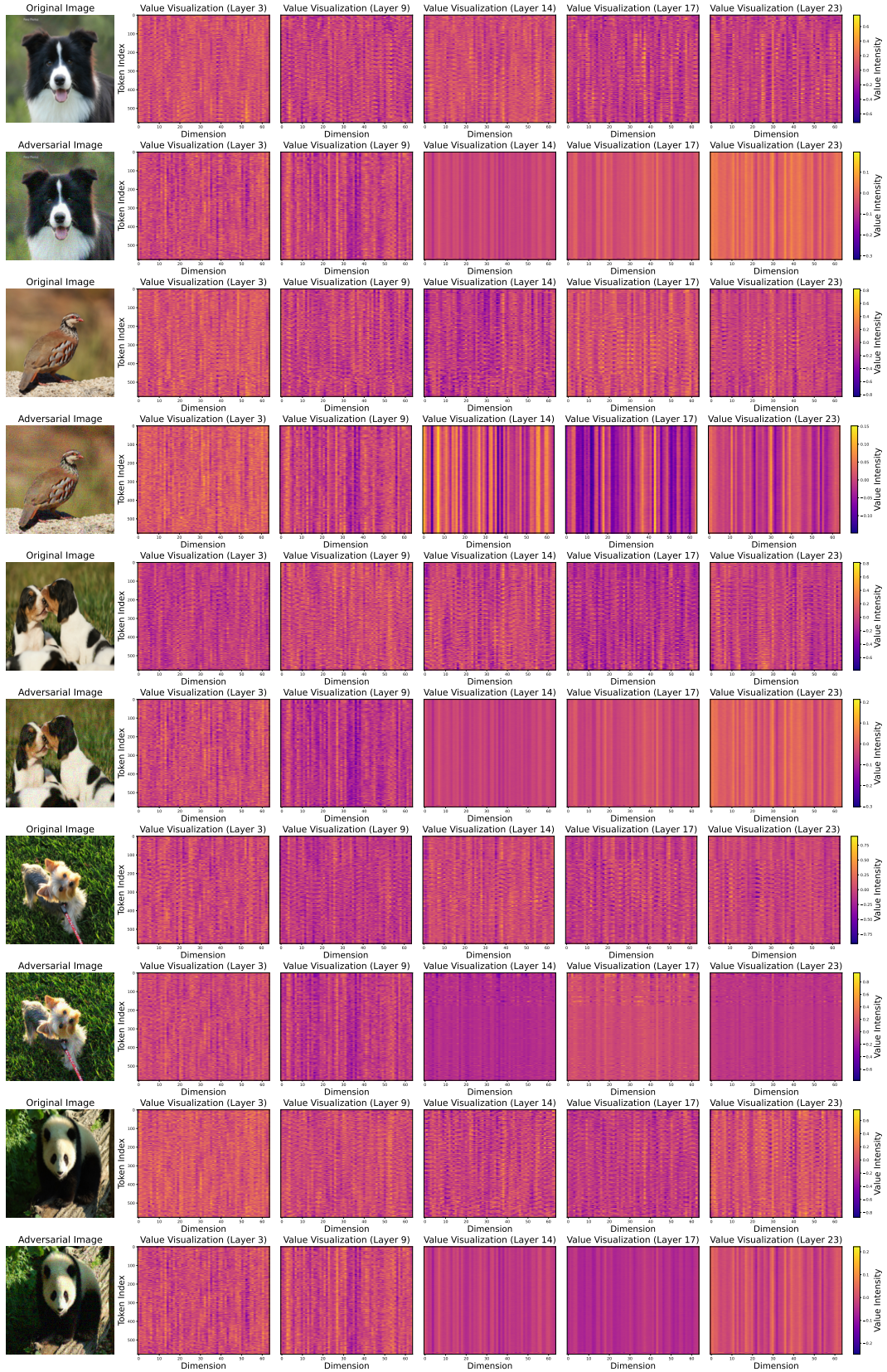


Figure 15. **Visualization of original and adversarial value vectors (CLIP-336).** The upper row displays the original image and corresponding value vectors across layers. The lower row shows the adversarial image applied with Doubly-UAP and its corresponding value vectors. Adversarial value vectors exhibit significant distortion compared to the original value vectors, showing vertical stripe patterns.

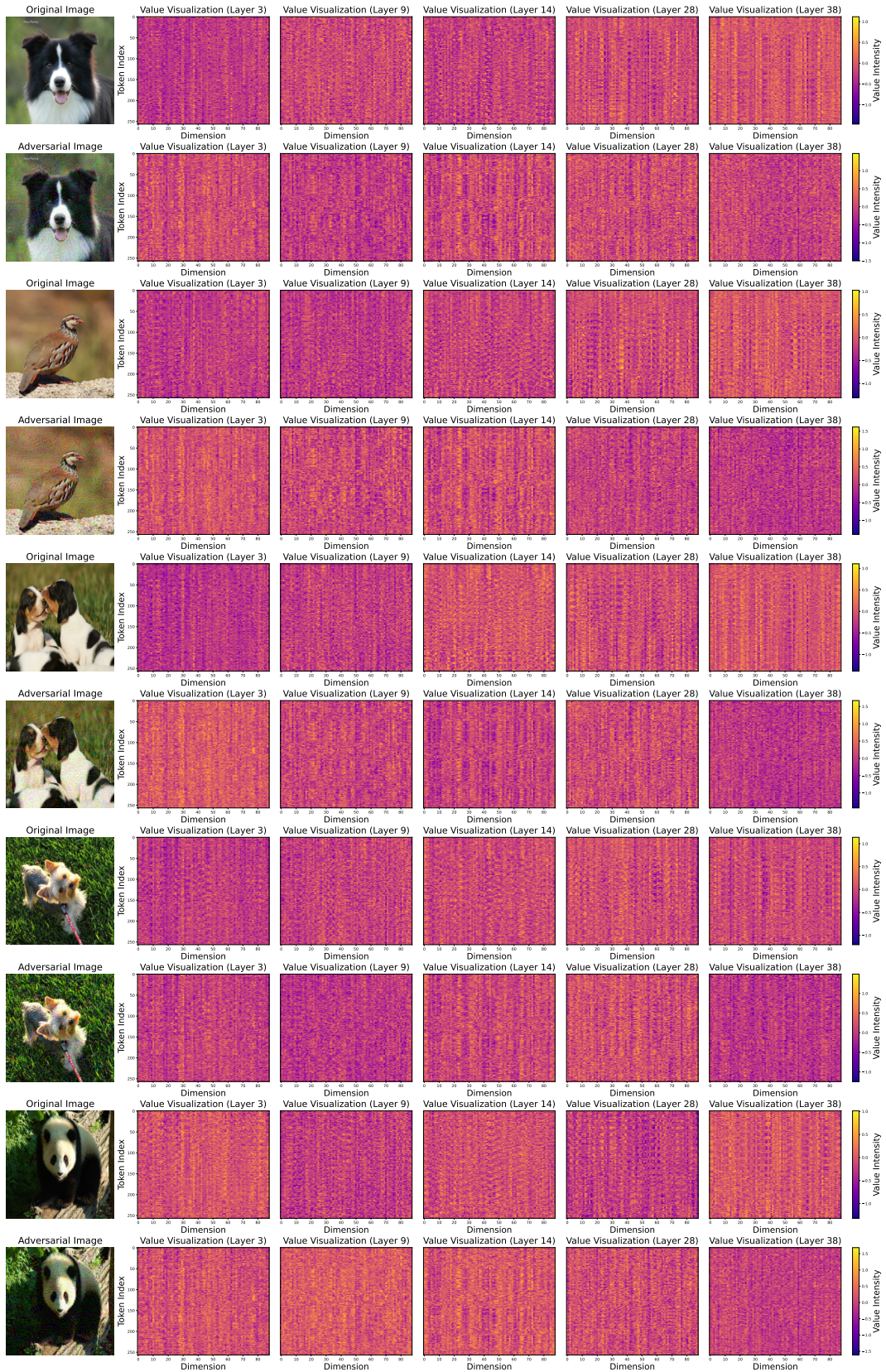


Figure 16. Visualization of original and adversarial value vectors in EVA-CLIP. The upper row shows the original image and its corresponding value vectors across layers, while the lower row displays the adversarial image perturbed by Doubly-UAP and its corresponding value vectors. The adversarial value vectors exhibit noticeable distortion compared to the original ones, losing their inherent patterns.